Modeling of Nonlinear and Non-stationary Multi-vortex Behavior of Electronic Crystals in Restricted Geometries of Nano Junctions

Tianyou Yi, Yulang Luo and Serguei Brazovskii
LPTMS-CNRS UMR 8628, Université Paris-Sud bat. 100 F-91405 Orsay, France
Corresponding author: T. Yi, email address: tianyou.yi@lptms.u-psud.fr

Abstract: Synthetic conductors show a phenomenon of periodic aggregation of electrons that is known as Electronic Crystals (EC). A common form of EC is the Charge Density Wave (CDW) with its spectral gap 2Δ, which determines optical and electronic properties of the materials. A recent technique of nano-scale junctions – Fig.2, fabricated by focused ion beams reveals a surprising feature in the tunneling spectra: the threshold gap which is ten times smaller than 2Δ, and followed by sequences of peaks appearing at higher voltages [1]. We witness the reconstruction of the electronic state under the applied field by proliferations of dislocations – CDW vortices. COMSOL allowed us to model the appearance of these patterns both in stationary states and in transient dynamics. This challenging problem requires solving multi-field nonlinear partial differential equations in 2+1 space-time dimensions. The variables are the two components of the CDW complex order parameter, the electric potential, and – for the liquid part of the electrons: the concentration, the current and the chemical potential.

Keywords: electronic crystal, charge density wave, nano-junction, field-effect, dislocation, vortex.

1. Introduction

The charge density wave (CDW) is a kind of electronic crystal [2] which phase transition is formed spontaneously by electron—lattice interaction through the symmetry breaking, thus forming a volatile state which can be locally affected by electrons' injection. Under an applied electric field in a constraint geometry, the CDW will experience stress which is resolved by the ground state reconstruction, and these processes go via creation of topological defects like solitons and dislocations—the CDW vortices [3,4] Fig. 1. In this article, we present a model of internal reconstruction in the CDW junction. We take into account multiple fields in mutual nonlinear interactions: the phase and the amplitude of the CDW order parameter, distributions of the electric potential, of the density and the current of normal carriers. The dissipative equations have been solved numerically by the time-dependent solver of COMSOL Multiphysics 3.5a. With a finite element method, we could successively handle the complex real shape of the junction in two spatial dimensions. Furthermore, the COMSOL code offers an easy and efficient implementation of the model consisting of four coupled strongly nonlinear partial differential equations. The numerical work was performed for parameters close to experiments on the inter-layer tunneling in NbSe3 [1].

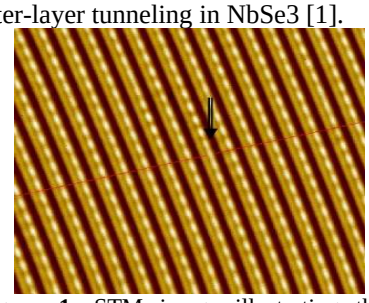

Figure 1. STM image illustrating the periodic modulation of electronic density for CDW in $NbSe_3$ [5]. Arrow points to the topological defect, where the CDW amplitude passes zero and the phase winds by 2π, which is the subject studied in this paper.

We have accessed the dynamical behavior of the penetrating vortices into the CDW and illustrated their final pattern formation. The numerical results correspond well to the experimental observations.

2. Model

Charge density wave exists in many quasi-one dimensional materials. Under the CDW transition temperature, the electrons condensate to form CDW chains, see Fig. 1. It is a self-consistent periodic deformation of both the electronic density and lattice distortion, which is nearly sinusoidal ~ $A\cos(Qx+\varphi)$. Hence, it can be described by the complex order parameter $\Psi=Ae^{i\varphi}$ given by the amplitude A, which is proportional to the energy gap Δ, and the phase φ. Working with the complex field Ψ allows us to study the

formation of topological defects like vortices—the ICDW dislocations. The phase φ characterizes the ground state degeneracy, while its distortions form the collective mode. Phase increment by 2π adds one CDW period thus concentrating the charge 2e, and therefore the charge density (per chain unit length) is $n_{CDW} = \frac{e}{\pi}A^2\varphi'$, with $\varphi' = \partial_x\varphi$ being the phase gradient alone the chain direction X.

The model should deal with intricate distributions of the order parameter Ψ, electric potential Φ, the normal charge density n and the normal current j.

We use the time-dependent dissipative Ginsburg-Landau approach to describe the dynamics of the CDW system. The static state is determined by a minimization of the total energy functional $H_{total} = H_{CDW}(\Psi) + H_{el}(\Phi)$. The CDW free energy H_{CDW} can be written as:

$$H_{CDW} = \int d\,r^3 \left\{ \frac{\Delta\xi}{4\pi s}\left(|\partial_x\Psi|^2 + \beta^2\left|\partial_y\Psi\right|^2\right) + \frac{\Delta}{2\xi s}|\Psi|^2 \ln\left(\frac{|\Psi|^2}{e}\right)\right\}. \quad (1)$$

Here Δ is the CDW gap, ξ is the correlation length $\xi=\hbar v_F/\Delta$, *s* is the unite area per chain, v_F is Fermi velocity of the parent metal. The first two terms give the energy of elastic deformation: compression and shear; β~0.1 is the parameter of the structural anisotropy. The third term is the CDW ground state energy, with a minimum at |Ψ|=1, with Ψ normalized to its equilibrium value.

The model also considers the local Coulomb interactions, which become very important since charges are concentrated near the vortex cores. H_{el} describes the effect of the local electric field, and of the free carriers with density n:

$$H_{el} = \int dr^3 \left(\frac{\Phi}{s}\frac{A^2}{\pi}\partial_x\varphi + \Phi\frac{n(\zeta)-\bar{n}}{d_a} - \frac{\varepsilon}{8\pi}|\nabla\Phi|^2\right) + F(n), \quad (2)$$

where potential Φ is assumed to incorporate the one-electron charge $e > 0$.

Here $n(\zeta) = \frac{n_0 T}{\varepsilon_F}\ln(1 + e^{\frac{\varepsilon_F+\zeta}{T}})$

is the local density per area in the single plane (n_0 is its unperturbed value at T=0 and ζ=0), d_a is the inter-plane distance and ε~10 is the host dielectric constant. The first and the second terms in (2) give the interaction of the collective and the normal charges with the electric field, the third terms is the field energy. The last term F(n) is the free energy of carriers giving the definition of the local chemical potential $\zeta=\partial F/\partial n$.

The system evolution is governed by dissipative equations of the order parameters:

$$-\gamma_A\frac{\partial A}{\partial t} = \frac{\delta H_{CDW}}{\delta A}, \quad (3)$$

$$-\gamma_\varphi\frac{\partial \varphi}{\partial t} = \frac{\delta H_{CDW}}{\delta \varphi}, \quad (4)$$

and the Poison equation for the electric potential Φ,

$$\frac{\varepsilon}{4\pi}\nabla^2\Phi = -\frac{A^2}{\pi s}\partial_x\varphi - (n(\zeta)-\bar{n}). \quad (5)$$

Here $\gamma_{A,\varphi}$ are the damping coefficients and can be executed from independent experimental measurement $\gamma_\varphi \sim 10^8$ energy/(m^3·second). The relaxation time for the amplitude A is much shorter than the for the phase φ, then we can approximately put $\gamma_A \approx 0$, so that the energy is always minimum with respect to A.

The equations have to be completed by the diffusion equation for normal carriers n:

$$\frac{\partial n}{\partial t} + \nabla \mathrm{j} = \frac{\partial n}{\partial t} - \nabla\left(\hat{\sigma}\nabla(\zeta+\Phi)\right) = 0, \quad (7)$$

with $\hat{\sigma}$ the anisotropic conductivity tensor, which is taken to be proportional to the carriers' concentration n. The conductivity along the CDW chain direction can be 100 times larger than that along the other directions.

The boundary conditions reflect the following properties:

1. CDW stress vanishes at all boundaries $\left(\frac{\Delta\xi}{2}A^2\nabla\varphi - A^2\Phi\vec{x}\right)\cdot\vec{\nu} = 0$; $(\frac{\Delta\xi}{2\pi s}\nabla A)\cdot\vec{\nu} = 0$.
2. Normal electric field is zero at all boundaries meaning the total electro-neutrality and the confinement of the electric potential within the sample: $\left(\frac{\varepsilon}{4\pi}\nabla\Phi\right)\cdot\vec{\nu} = 0$.
3. No normal current flow through the boundaries such that $-\hat{\sigma}\frac{n}{n_0}\nabla(\zeta+\Phi) = 0$, except for the two source/drain boundaries left for the applied voltage. There, the chemical potentials are applied: $\zeta + \Phi = \pm V$.

In the above equations $\vec{x}$ is the unit vector along the chain axis, $\vec{\nu}$ is the outward unit normal vector on the domain.

3. Numerical Method

The geometry design of our model based on the real experimental junction is shown in Fig. 2 with two overlapping cuts across the sample. The junction made from CDW material is of high isotropic conductivity,

where normally the current goes along the high conductivity direction. However, the two slits cut enforce the current to go the traverses direction Y of high resistivity providing the original strong voltage drop at the central rectangular region. We did simulations for two different geometries: first the simplified geometry—the central rectangular region of the junction, and second the full real geometry—the restricted geometry junction.

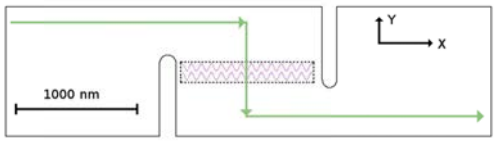

Figure 2. Sketch of the real geometry of the junction, and its active rectangular center part where the vortices can stay. The green arrows indicate the direction of the normal current flow.

For the real geometry, the equation system is valid in the body of the junction. However, in the two slits there is neither condensate nor normal electrons, we solve only the Laplace equation for Φ there ($\Delta\Phi=0$). We adopt the marching boundary conditions (Neumann boundary condition) for Φ along the slit boundaries.

The initial conditions are chosen to be $|\Psi|=1$ and with zero electric field in the body of the junction. In view of the complicated geometry, we have chosen an implementation of the model in COMSOL using quadratic Lagrange elements, which turned out to give sufficiently accurate and stable solutions. The complex order is separated into its real part and imaginary part $\Psi=u+iv$, and their equations written in the general form in COMSOL. The number of degree of freedom is about $2\cdot10^5$, and the mesh density was 7nm by 7nm in the most dense center region, which was enough to obtain the high-resolution results, for the typical size of the vortex is about 50nm. Programs are run on a 4-core Xeon workstation, and the computation time is about 3 hours for the simple geometry and about 6 hours for complex geometry.

4. Results and Discussion

Below we present the results for two different geometries of the junction: first the simplified geometry—the central rectangular region of the junction, and second the real geometry—the restricted geometry junction. The temperature was taken at about 50K—below the CDW transition temperature 59K for $NbSe_3$.

Two types of DLs have been revealed by the simulation: a dynamic vortex, and a stationary one. The dynamic vortices appear through the early evolution after the voltage application, and they disappear at the end. The stationary vortices appear later and they reach the equilibrium configuration.

Two regimes of the CDW vortex formation have been observed during the simulation. The initial regime in Figs.3 and 4 with the characteristic time 10^{-11} second (which is at the boundary of our dissipative approximation) is the transient, turbulent one. During this time, the flashes of zero CDW amplitude appear at the sample boundaries, evolving into well-structured vortex cores. In addition, the annihilation between two vortices of opposite sign and destruction of vortices near boundaries are observed. The number of vortices participating in the transient process is much larger than that left in the stationary state. In the second regime, the remnant vortices move slowly to find their equilibrium positions. Finally, at time about 10^{-6} to 10^{-5} second the system relaxes into equilibrium and a true vortex stationary state is achieved. The whole evolution of the system from the first regime to the second regime can be seen in the movie (available at site).

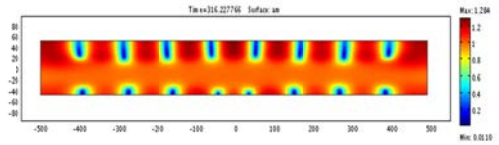

Figure 3. Image snapshot of vortex traces showing an intermediate state of vortex formation in the rectangular geometry. Color varying from red to blue corresponds to the range of amplitude from 1 to 0.

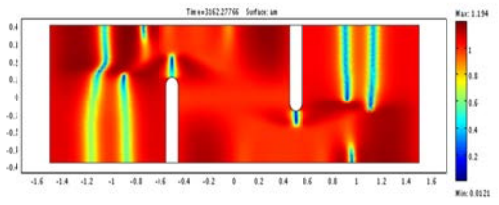

Figure 4. Image snapshot of vortex traces showing an intermediate state of vortex formation in the junction.

An idealized analytic theory [6, 7] predicts that there exists a threshold voltage for appearance of the vortices. It is to point out that the fundamental origin of the threshold

energy can be related with the breaking of interlayer CDW coherency. For this to happen it requires a critical voltage difference $\delta V_{CR} \sim (\hbar v_F J_z)^{1/2}$ which depends on the inter-chain coupling energy (per unit length) J_z. For the rectangle geometry and for realistically chosen parameters, we have obtained that the first stationary vortex appears at $V=0.308\Delta$ (7.7meV). The second stationary vortex appears at $V=0.328\Delta$ (8.2meV), the third one at $V=0.376\Delta$, and the forth one at $V=0.568\Delta$ see Fig. 5. For the real geometry, the first stationary vortex appears at $V=0.268\Delta$ (6.7meV) and the second stationary vortex appears at $V=0.32\Delta$ (8meV) see Fig. 6. We find that the number of the stationary vortex augments with the applied voltage.

As shown in Figs. 5 and 6 the CDW amplitude vanishes continuously at the vortex cores (in blue color), while it remains nearly unperturbed and closed to its normalized value 1 (in red) for the major part of the junction. The conversion of the CDW condensate electrons to the normal electrons may happen at the vortex cores, where the CDW state is destroyed.

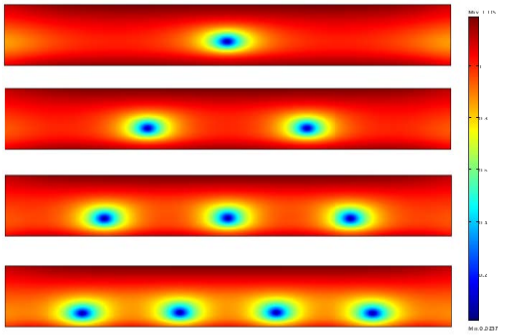

Figure 5. Formation of vortices in the rectangle center of the junction. The number of vortex increases with the applied voltage: V = 0.308Δ, 0.328Δ, 0.376Δ, 0.568Δ, respectively.

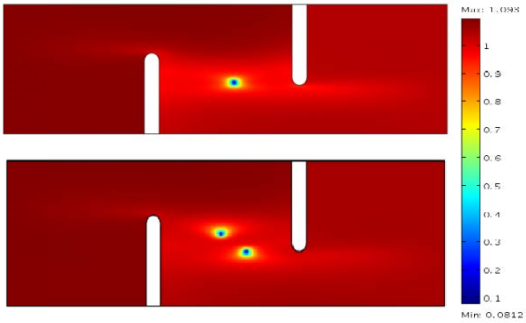

Figure 6. Formation of vortices in the real junction. The number of vortex increases with the applied voltage V=0.268Δ, 0.32Δ, respectively.

The phase winds by 2π around the cortex core (Figs. 7 and 8), which becomes the center of phase slip. The plots of the amplitude and the phase give us a way to identify and visualizer the topological defects.

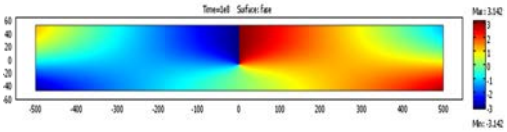

Figure 7. In the rectangle geometry, the phase rotates by 2π around the vortex core. In the color map, the phase passes form π in red to $-\pi$ in blue.

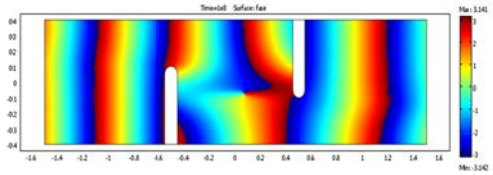

Figure 8. The same 2π circulation of the phase around the vortex core in the center for the real geometry.

Distribution of the electric potential Φ at the presence of one vortex is given at Fig. 9 (the rectangle geometry) and Fig. 10 (the real geometry). The total electric charge at the vortex core is zero, but the electric dipole moment is built-in, thus inducing the electric field resulting in a sharp drop of Φ at the vortex core. This should increase the tunneling probability of electrons near the core, which explains the peaks observed in experimental tunneling spectra.

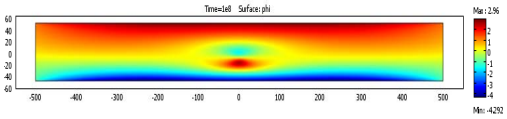

Figure 9. Electric potential Φ for the one-vortex state in the rectangle geometry. The sharp variation of Φ is confined within the vortex core. Notice the sign inversion of Φ across the core.

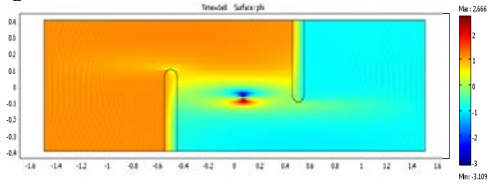

Figure 10. The same electric potential Φ for the one-vortex state in the real geometry.

7. Conclusions

We have performed a program of modeling the stationary states and their transient dynamic for the CDW in restricted geometry junction by COMSOL. We used COMSOL to study the microscopic properties of electronic correlated materials, and our results give access to stationary and transient processes at nano-scale in space and pico-second scale in time.

Spontaneous vortex formation is observed above a critical value for the applied voltage. The critical voltage is identified as the dislocation line entry energy, in some analogy to the H_{C1} field in superconductivity. A sharp drop of the electric potential across the vortex cores can lead to enhanced inter-layer tunneling, which explains the observed peaks in experimental tunneling spectra.

The studies of reconstruction in junction for the CDW vortex state can be relevant to modern efforts of the field-effect transformation in strongly correlated materials that also show a spontaneous symmetry breaking.

8. References

1. Yu. I. Latyshev, P. Monceau, S. Brazovskii, A. P. Orlov, and T. Fournier, Subgap Collective Tunneling and Its Staircase Structure in Charge Density Waves, *Phys. Rev. Lett.*, **96**, 116402 (2006)

2. Proceeding of the International Workshops on Electronic Crystals –ECRYS 2008, S. Brazovskii, N. Kirova and P. Monceau Eds. *Physica B*, **404**, (2009)

3. S. Brazovskii, Solitons and Their Arrays: From Quasi 1D Conductors to Stripes, *Journal of Superconductivity and Novel Magnetism*, **20**, 489-493 (2007)

4. S. Brazovskii, in [1] p. 482-486

5. Brun, C., Wang, Z.-Z., Monceau, P., Scanning tunneling microscopy at the $NbSe_3$ surface: Evidence for interaction between q_1 and q_2 charge density waves in the pinned regime, *Phys. Rev. B*, **80**, 045423, (2009)

6. S.A. Brazovskii, S.I. Matveenko, Dislocations in Charge Density Wave Crystals, *Sov. Phys. JETP*, **72**, 860, (1991)

7. S.A. Brazovskii, S.I. Matveenko, Charged Density Wave Structure Near Contacts, *Sov. Phys. JETP*, **74**, 864, (1992)